Available online at www.sciencedirect.com
SCIENCE DIRECT®
Journal of Photochemistry and Photobiology A: Chemistry 164 (2004) 129–135
Journal of Photochemistry and Photobiology A:Chemistry
www.elsevier.com/locate/jphotochem

Application of an ionic liquid-based electrolyte to a 100 mm × 100 mm sized dye-sensitized solar cell

Hiroshi Matsui [a,*], Kenichi Okada [a], Takuya Kawashima [a], Tetsuya Ezure [a], Nobuo Tanabe [a], Ryuji Kawano [b], Masayoshi Watanabe [b]

[a] *Material Technology Laboratory, Fujikura Ltd., 1-5-1 Kiba, Koto-ku, Tokyo 135-8512, Japan*
[b] *Department of Chemistry and Biotechnology, Yokohama National University, 79-5 Tokiwadai, Hodogaya-ku, Yokohama 240-8501, Japan*

Received 25 July 2003; received in revised form 1 December 2003; accepted 14 December 2003

Abstract

In this study, an ionic liquid-based electrolyte was applied to a 100 mm × 100 mm sized dye-sensitized solar cell (DSC). For the purpose of fabricating a large sized DSC, influence of electrode distance, TiO_2 nano-particle size, thickness of TiO_2 nano-porous layer were investigated in ionic liquid; 1-ethyl-3-methylimidazolium bis(trifluoromethanesulfonyl)amide (EMIm–TFSA) electrolyte system. It was cleared that short-circuit current (J_{sc}) was remarkably influenced by those factors compared with conventional volatile electrolyte system. At optimized condition, energy conversion efficiency of 4.5% was obtained using 9 mm × 5 mm small sized cell. Energy conversion efficiency of a large sized cell was 2.7% on ionic liquid system, and 2.4% on ion–gel system based on the active area (2.3 and 2.0%, respectively, based on the total area). Cell performance was drastically improved by decreasing of internal cell resistance, mainly attributed to conductivity of a transparent conductive oxide (TCO) substrate.

Keywords: Dye-sensitized solar cell; Ionic liquid; Ion–gel; TiO_2

1. Introduction

Because of low fabrication costs, simple manufacturing process, using no toxic materials and so on, a dye-sensitized solar cell (DSC) composed of nano-crystalline TiO_2, organic dyes and an electrolyte [1] is expected to be a large-scale prevalent solar cell. The cell usually employs an electrolyte including I^-/I_3^- redox couples dissolved in a volatile organic solvent such as acetonitrile. For its practical use, it is necessary to prevent electrolyte from evaporation of a solvent. During long-term operation, solvent losses occur owing to its high volatility resulting in decreasing of cell performance. There are many researches to improve cell stability by replacing such an electrolyte with non-volatile one. As one of those researches, an ionic liquid seems to be suitable for an electrolyte of the cell. An ionic liquid has unique properties such as non-volatility, non-flammability and electrochemical stability, so that utilization in a wide range of electrochemical devices like batteries has been expected. Various ionic liquids have been studied as electrolyte materials for DSC since their first report [2], and especially, those with 1,3-dialkylimidazolium cations were used well. It was reported that cells applied ionic liquids displayed good long term and thermal stability [2,3]. On the other hand, in an ionic liquid electrolyte, physical mass transfer is slower than that in a conventional volatile electrolyte, because it is highly viscous [5]. Hence, for ionic liquid type DSC, it is necessary to increase generation output and to develop to penetrate electrolyte solution into nano-porous layer uniformly. For an ionic liquid type electrolyte, a unique charge transport process, not only by simple physical diffusion, was proposed [2,6,7]. Watanabe and co-wokers reported a significant enhancement of charge transport rate in some particular condition of iodine redox composition owing to conjugation of physical diffusion and exchange reaction in the ionic liquid [6,7].

Moreover, for the practical use, solidification of an electrolyte layer is expected to prevent electrolyte leakage when a cell is broken or a cell is in the manufacturing process. An ion–gel electrolyte that was gelated an ionic liquid chemically or physically by using of proper gelator have been extensively studied [3,4,8–11]. Yanagida and co-workers investigated a property of an ion–gel electrolyte closely using low molecular gelator, and showed remarkable improvements of cell stability [3,4]. Upscaling

* Corresponding author. Tel.: +81-3-5606-1067; fax: +81-3-5606-1511.
E-mail address: matsui@rd.fujikura.co.jp (H. Matsui).

1010-6030/$ – see front matter © 2004 Elsevier B.V. All rights reserved.
doi:10.1016/j.jphotochem.2003.12.022

technology of a cell that has laboratory size onto practical size is also needed. For the enlargement, it is important that a decreasing of an IR drop attributed to an internal resistance of the cell that will increase significantly with expanding of a photoelectrode area. Two kinds of approaches have been reported that is by a combination of many cells or by enlargement of a unit cell area [12,13]. To realize a high-performance DSC, overcoming of these subject matters must be indispensable. Especially, for an ionic liquid system, a cautious design of dimensional conditions of an electrode is required because it is considered that factors such as mass transfer length in the electrolyte layer affect cell performance more serious than that in a conventional volatile electrolyte system. In this study, we fabricated large sized cells using an ionic liquid electrolyte through an optimization of cell preparation conditions for our ionic liquid system and an investigation of an ion–gel electrolyte for the sake of a development of a practical DSC.

2. Experimental

2.1. Sample preparation

An ionic liquid, 1-ethyl-3-methylimidazolium bis(trifluoromethanesulfonyl)amide (EMIm–TFSA as shown in Fig. 1) was used. An electrolyte solution using EMIm–TFSA (simply called as "ionic liquid electrolyte" hereafter) was composed of 1.5 mol/l of 1-ethyl-3-methylimidazolium iodide (EMIm-I), 0.15 mol/l of I_2, 0.1 mol/l of LiI, and 0.5 mol/l of 4-*tert*-butylpyridine (TBP) that was dissolved in EMIm–TFSA. EMIm–TFSA was prepared by an anion exchange reaction from 1-ethyl-3-methylimidazolium bromide (EMIm-Br) and bis(trifluoromethanesulfonyl)amide lithium salt (Fluka Chemical). EMIm-I and EMIm-Br was synthesized from 1-methylimidazole and bromoethane or iodoethane, respectively. Small amount of water, less than 1 wt.%, was added to the electrolyte solution before measurement. An electrolyte solution using a volatile solvent (simply called as "volatile electrolyte" hereafter), as a reference, was composed of 0.3 mol/l of 1,2-dimethyl-3-propylimidazolium iodide (Shikoku Corporation), 0.05 mol/l of I_2, 0.1 mol/l of LiI, and 0.5 mol/l of TBP that was dissolved in methoxyacetonitrile. For preparation of an ion–gel electrolyte, poly(vinylidenefluoride-*co*-hexafluoropropylene) (PVdF–HFP) (Kynar 2751, Atofina Japan, formerly Elf Atochem Japan) and the ionic liquid electrolyte were dissolved in tetrahydrofuran. By casting this solution, the ion–gel electrolyte was packed into an intervening space between photo and counter-electrode. PVdF–HFP content in the ion–gel electrolyte was 8 wt.%.

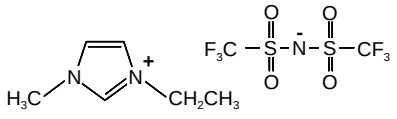

Fig. 1. Structure of an ionic liquid: 1-ethyl-3-methylimidazolium bis(trifluoromethanesulfonyl)amide (EMIm–TFSA).

A photoelectrode, which had 9 mm × 5 mm area for a small sized cell, was prepared as follows. A TiO_2 paste was coated on a sheet glass substrate with a transparent conductive oxide (TCO) layer using a doctor-blade technique. Nanoxide-T (Solaronix) was used as the TiO_2 paste for a standard condition. A different TiO_2 paste was also used for evaluation of influence of particle size toward cell performance. TiO_2 particles for latter were synthesized from titanium tetraisopropoxide and acetylacetone, and the paste was prepared based on a reported procedure [14]. A fluorine-doped stannic oxide (FTO) was used as the TCO (8–10 Ω/sq). After drying the wet film on the substrate, the film was sintering at 450 °C. A light reflecting layer consist of large size TiO_2 particles (HPW-400C, Catalysts&Chemicals Ind.) was prepared over the nano-porous TiO_2 layer using same procedure. Sintering time was totally 60 min.

In the case of preparation of a photoelectrode for a 100 mm × 100 mm large sized cell, mixture of two kinds of TiO_2 pastes that consisted of Nanoxide-T and another one (mixing ratio was 8:2) was used for depressing delamination of a TiO_2 film. The latter paste was prepared based on the reported procedure using TiO_2 particles; P25 (Nippon Aerosil) [14]. A TCO substrate for the large sized cell had an FTO/ITO double layer and current collecting grids on a sheet glass substrate for decreasing resistance. Current collecting grids were directly formed on a TEMPAX #8330 glass substrate by means of additive process for printed wiring boards (to be published). Concretely describing, a template for grids was formed by using a photosensitive dry film. After that, as current collecting grids, a nickel metal layer was electrodeposited on the substrate having a chromium seed layer. The FTO/ITO layer was prepared by spray pyrolysis deposition method (2–3 Ω/sq) [15] onto glass substrate formed grids. Deposition of an ITO layer was carried out using an ethanol solution of $InCl_3{\cdot}4H_2O$ and $SnCl_2{\cdot}2H_2O$ on a substrate of 350 °C, and an FTO layer was consecutively deposited over the ITO layer from an ethanol/water solution of $SnCl_4{\cdot}5H_2O$ and NH_4F at a substrate temperature of 400 °C.

The substrate with the TiO_2 layer was immersed overnight in a solution of a dye (ruthenium (2,2′-bipyridyl-4,4′-dicarboxylate)$_2$ $(NCS)_2$ as called N3 Dye) (Kojima Chemicals or Solaronix S.A.) at room temperature. As a counter-electrode, the TCO substrate on which platinum had been deposited by sputtering was used.

In preparation of test cells, a photo and a counter-electrode were clamped together and the intervening space between two electrodes was filled with an electrolyte by casting a droplet. Distance between two electrodes was fixed by polymer sheets (Teflon or Himilan) of various thicknesses putting around TiO_2 nano-porous layer region on the photoelectrode substrate. In the case of zero thickness spacer, each electrode was directly clamped.

2.2. Measurement

Measurement of the *I–V* characteristics of cells was carried out using a potentiostat/galvanostat (SI1286, Solartron, formerly Schlumberger) and a dc electronic load (MP-160, Eiko Seiki) under simulated solar light (AM 1.5, 100 mW/cm^2, ESS-150A, Eiko Seiki). TiO_2 particles were observed by a field-emission type scanning electron microscope (FE-SEM) (S-5200, Hitachi). The crystal structure of TiO_2 particles was determined by X-ray diffraction using Cu Kα radiation (RAD-1C, Rigaku). The BET surface area was measured by a surface area analyzer (GEMINI 2360, Shimadzu).

3. Results and discussion

3.1. Influence of cell fabrication conditions to EMIm–TFSA system

As shown in Fig. 2, apparent diffusion coefficients of I^-/I_3^- in ionic liquids were smaller than that in a volatile electrolyte solution because of their high viscosity. It was reported that a high-rate charge transport with an exchange reaction was prominent when concentration of the redox species was high and, in addition, that of I^- and I_3^- were comparable [6,7]. In such an electrolyte composition, however, influence of incident light absorption by I_3^- was also significant. Therefore, at this time, experimental cell performance in this system was favorable in the composition including high redox species concentration compared with a volatile electrolyte system and low ratio of I_3^- [16]. It is considered that physical diffusion of redox species mainly contributed to charge transport in such a cell. Consequently, it must be important to design cell elements to be able to decrease influence attributed to slower diffusion in the electrolyte solution.

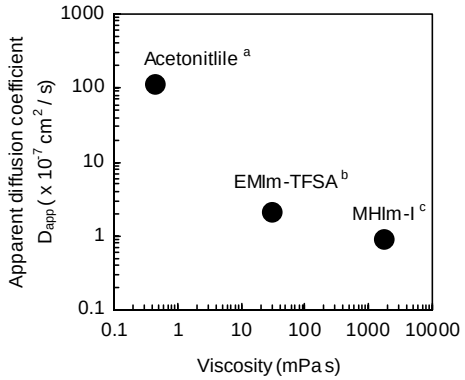

[a] From ref. [5]

[b] The electrolyte solution; EMIm-I (1 mol/l) : I_2 = 10 : 1 dissolved in EMIm-TFSA [6,7]

[c] The electrolyte solution; 0.04 mol/l I_2 dissolved in methyl-hexyl-imidazolium iodide [2]

Fig. 2. Comparison of viscosities and apparent diffusion coefficients between various electrolyte systems.

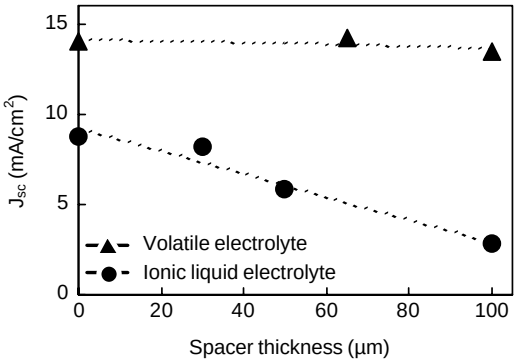

Fig. 3. Dependence of short-circuit current density, J_{sc} of cells on a spacer thickness obtained by two kinds of electrolyte systems.

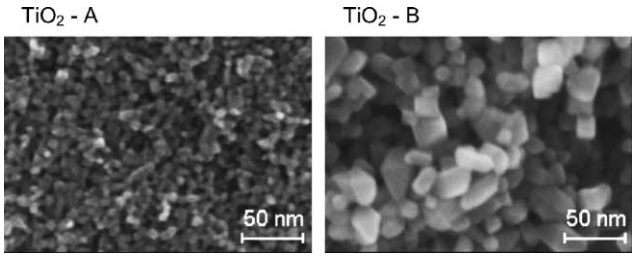

Fig. 4. FE-SEM images of nano-crystalline TiO_2 particles used in this study.

Fig. 3 shows dependence of short-circuit current (J_{sc}) on a thickness of spacer (in other words, distance between two electrode substrates). J_{sc} remarkably decreased with increasing distance between two electrodes compared with the cell using a volatile electrolyte, and it was found that the thickness of the electrolyte layer affected significantly energy conversion efficiency in this cell system. Furthermore, mobility of species was very restricted within the nano-pores of a TiO_2 layer. It was reported that an effective diffusion constant for I_3^- in the nano-porous TiO_2 layer was significantly lower than the bulk value [17]. Influence of a particle size of TiO_2 and a thickness of TiO_2 layer on a cell characteristic was investigated. Two kinds of TiO_2 particles were used for experiment as shown in Fig. 4 and Table 1. Dependence of J_{sc} on a thickness of nano-porous TiO_2 layers evaluated by using different sized TiO_2 particles was shown in Fig. 5. In the case of cells using smaller size TiO_2 particles; TiO_2-A, large BET surface area of those TiO_2 layers brought large amount of molecular dyes absorbed on particles although

Table 1
Comparison of nano-crystalline TiO_2 particles used in this study

	Synthesized particles (TiO_2-A)	From nanoxide-T (TiO_2-B)
Crystal structure	Anatase	Anatase
Particle size (nm)	∅ 6–9	∅ 13–20
BET surface area (g/m^2)	220	80

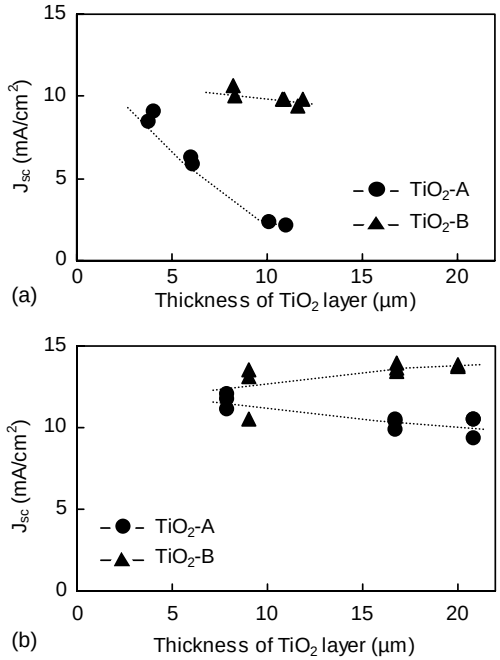

Fig. 5. Dependence of short-circuit current density, J_{sc} on a thickness of a nano-porous TiO_2 layer: (a) in an ionic liquid electrolyte system; (b) in a volatile electrolyte system.

the thickness was thin, so that J_{sc} value was comparatively large in thin region of the thickness. However, J_{sc} notably decreased with increasing film thickness. It was considered that, especially in the viscous ionic liquid electrolyte system, significant inhibition of I^-/I_3^- transport caused the decreasing of J_{sc} with increasing of the TiO_2 layer thickness (i.e. increasing of mass transport length in the nano-porous film) because nano-pore size was too small in this film consisting TiO_2-A particles. On the other hand, J_{sc} obtained by a cell using larger size TiO_2 particle; TiO_2-B, was not showed such a drastic decreasing tendency. It showed only slight one. In the case of a system using a volatile electrolyte, such a decreasing of J_{sc} was not observed up to thicker layer in either particle using. As results, those factors about electrodes affect cell performance of the ionic liquid system seriously compared with that of the volatile electrolyte system, and appropriate condition was considerably different between two systems. It was necessary to secure shorter distance between photo and counter-electrodes, suitable layout of nano-porous TiO_2 films in which a transport of species was not remarkably inhibited for the ionic liquid electrolyte system.

In the case of addition of only iodine redox couples to EMIm–TFSA, open-circuit voltage; V_{oc} of a cell was very low compared with a volatile electrolyte system. It was considered that a difference of redox potential of an electrolyte solution and an increasing of recombination of electrons with I_3^- due to including dense iodine redox couples caused such a low V_{oc}. By addition of TBP [18] and lithium cation, it could be decreased dark current as shown in Fig. 6, and improved cell performance (Table 2). After the optimization

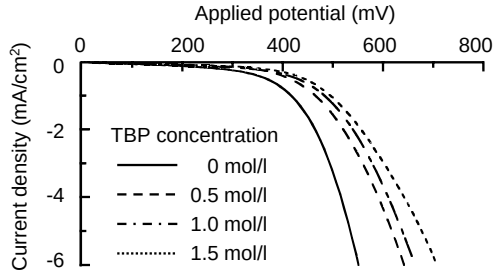

Fig. 6. Dark current characteristics of cells obtained by an ionic liquid electrolyte system including 0 mol/l (—), 0.5 mol/l (– – –), 1.0 mol/l (– · –) and 1.5 mol/l (- - -) of TBP.

Table 2
Photovoltaic characteristics of ionic liquid electrolyte type cells including various additives

	V_{oc} (mV)	J_{sc} (mA/cm^2)
Without additives	527	10.1
With TBP[a]	647	9.5
With TBP + LiI[b]	645	10.9

[a] TBP concentration was 0.5 mol/l.
[b] LiI concentration was 0.1 mol/l.

as mentioned above, 4.5% of energy conversion efficiency of 4.5% was obtained in a cell using EMIm–TFSA as shown in Fig. 7. Favorable photovoltaic characteristics were also reported by application of iodide salt type ionic liquids (e.g. MHIm-I) [3,4,8,11]. Those systems had advantageous for intentionally making of the exchange reaction between I^-/I_3^- because of its higher concentration. On the other hand, owing to hydrophobic nature and relatively lower viscosity, EMIm–TFSA system had practical advantages for avoidance of moisture adsorption, injection of an electrolyte into a cell and so on. At this time, the cell performance of this ionic liquid system has not beyond the one of conventional volatile electrolyte system. For increasing of energy conversion efficiency, it was considered that further improvement of electrolyte composition such as utilization of denser iodine redox region and thin electrolyte layer was necessary.

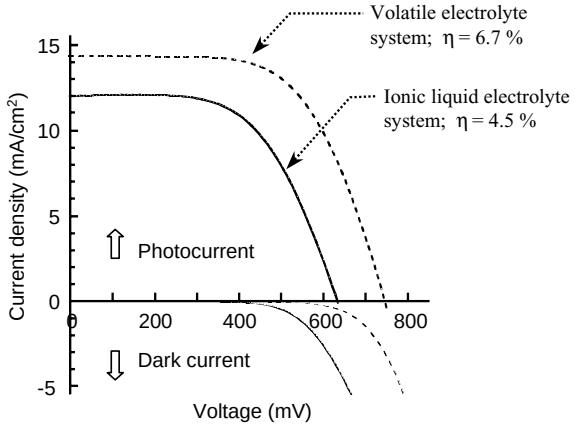

Fig. 7. *I–V* characteristics of cells using an ionic liquid electrolyte (—) and a volatile electrolyte (- - -). Photoelectrode size was 5 mm × 9 mm.

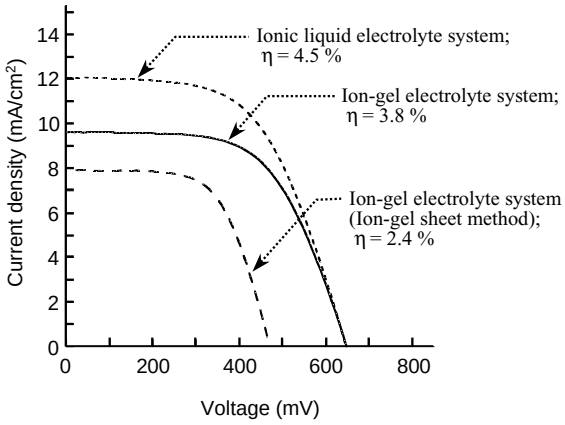

Fig. 8. *I–V* characteristics of cells using various type of electrolytes: ionic liquid electrolyte system (- - -); ion–gel electrolyte system (—); ion–gel electrolyte system prepared by ion–gel sheet method (– – –). Photoelectrode size was 5 mm × 9 mm.

3.2. Cell performance using ion–gel electrolyte

Quasi-solidification of the electrolyte solution was carried out using PVdF–HFP as a gelator. It was possible to form a stable ion–gel by addition of 5–8 wt.% gelator. Energy conversion efficiency of 3.8% was obtained in a 5 mm × 9 mm sized cell using the ion–gel electrolyte, and it was output about 85% compared with that of the ionic liquid type electrolyte system (Fig. 8). About 15% decreasing in efficiency was mainly based on decreasing of photocurrent. Probably, some pores, which were not filled up with electrolytes, were remained in the present cell.

Some distinctive applications of electrode structure or cell manufacturing are expectable by solidification of an electrolyte. In general, an electrolyte solution is injected into a cell through a small spout using capillary phenomenon, pressure difference and so on. In the case of an ionic liquid electrolyte, it is difficult to fill up all over the cell with electrolytes by conventional techniques since it is more viscous than a conventional volatile electrolyte. We developed a new cell fabrication process of ion–gel sheet method as shown in Fig. 9. An efficient manufacturing process by the roll-to-roll can be expected by the method in the future. For preparation of cells through this process, two electrodes were stuck each other sandwiching the ion–gel sheet, and penetration

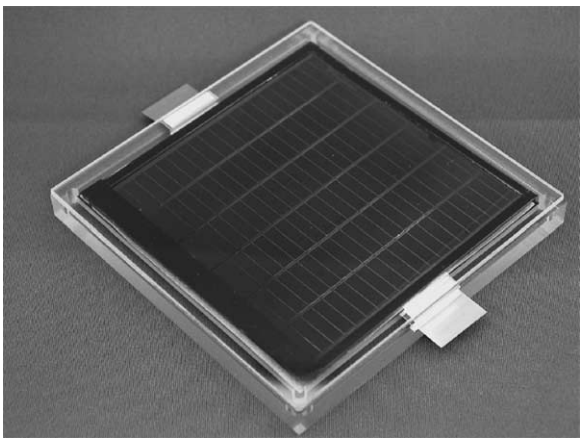

Fig. 10. A view of a fabricated 100 mm × 100 mm ionic liquid type DSC.

of an electrolyte was carried out by heat-press. Press condition was to load of 7 kgf/cm^2 and 60 min keep at 95 °C. After cooling, photo and counter-electrodes were apparently adhered mutually through the ion–gel electrolyte layer. As shown in Fig. 8, energy conversion efficiency obtained by the ion–gel sheet type cell was 2.4%. The ion–gel sheet process was successfully operated but photovoltaic output was relatively low compared with that of the ion–gel electrolyte type cell mentioned above. A prepared ion–gel sheet liquefied at an operation temperature of pressing process. Nonetheless, flowability of it might be poor, so that it was considered nano-pore of TiO_2 nano-porous film could not be uniformly filled with electrolyte.

3.3. Large sized DSC using an ionic liquid-based electrolyte

Based on results as mentioned above, 100 mm × 100 mm sized cell using EMIm–TFSA was fabricated (Fig. 10). For the practical use of DSC, it is necessary to enlarge cells to the size of several square centimeter or more at least without significant decreasing of cell performance. However, in particular, conductivity of a TCO layer on a glass substrate is not high enough, and only enlargement of a photoelectrode area results in decreasing cell performance significantly. Consequently, decreasing of internal resistance of a cell attributed to a TCO is indispensable.

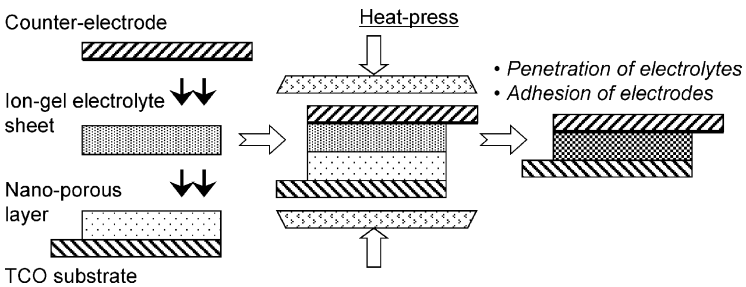

Fig. 9. Schematic drawing of a proposing cell manufacturing process with an ion–gel sheet.

TCO substrates for large sized cells need a property not only highly conductive but also passive against a reaction chemically and electrochemically with electrolytes including iodine redox couples. As such a TCO substrate, high-conductive transparent glass electrode with an FTO/ITO double layer and current collecting grids made of nickel was developed. The FTO/ITO double layer was composed of an ITO layer of ca. 700 nm thickness as the first layer and an FTO layer of ca. 100 nm thickness as the second layer. Current collecting grids were formed within the photoelectrode region as vertical five lines and crosswise 19 lines to a contact terminal side of the substrate. The thickness of grids was 2 μm on average. Similar current collecting nickel lines were also formed around the photoelectrode region. The area of a prepared photoelectrode was 81 cm (total area) and 85% of total area (i.e. 69 cm^2) was active area. Active area means a photoelectrode area that was not shaded incident light by current collecting grids. For avoiding directly contact with current collecting lines around the photoelectrode, a counter-electrode substrate had a size smaller than a high-conductive transparent glass electrode substrate.

Table 3 shows comparison of cell fabrication conditions between optimized small sized cells and prepared large sized cells. At this time, for large sized cells, the condition could not be perfectly identical with optimized results in small sized cells owing to several reasons about cell fabrication technique describing below. After sintering, nano-porous films consisted of TiO_2-B particles were peeled off in large area coating although good film was formed in small area coating. To improve this inconvenience, a different TiO_2 paste including P25 particles, which had adhesion superior to the paste for films mentioned above, was mixed with the original paste including TiO_2-B particles. Uniformity of film thickness should also be improved in the large photoelectrode area. Collaterally, the distance between photo and counter-electrodes might partially be different from that of optimized small sized cell even though each electrode was directly stacked. Fig. 11 and Table 4 show *I–V* characteristics obtained by large sized cells. Energy conversion efficiency was 2.7% on the ionic liquid system, and 2.4% on the ion–gel system based on the active area (2.3 and 2.0%, respectively, based on the total area). On the other hand, same size cell using a normal TCO substrate, which was not decreased resistance, worked very poor. In such a cell, a shape of *I–V* curve showed like straight line because of large internal resistance. As a result, it was found that a fabricated high-conductive transparent electrode could decrease internal resistance of the cell, and improved performance of large sized DSC. With regard to differences of conditions between the large sized cell and the small sized one described above, improvement of cell fabrication technique was needed hereafter. Through that, it was considered photovoltaic properties of large sized cells would be improved.

Table 3
Comparison of the cell fabrication condition between small sized cells and large sized cells

	Small sized cells	Large sized cells
TiO_2 particles	TiO_2-B	TiO_2-B + P25
Thickness of TiO_2 layer (μm)	8	6–8[a]
Photo and counter-electrodes stacking	Directly stacked	Directly stacked
Electrolyte	Same composition[b]	

[a] Thickness uniformity was incomplete.
[b] The composition was expressed in Section 2.1.

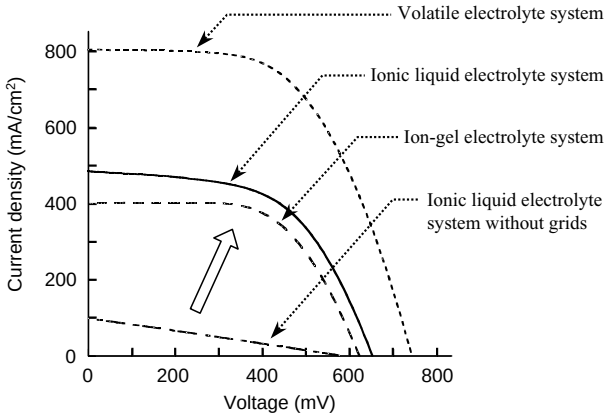

Fig. 11. *I–V* characteristics of large sized cells using an ionic liquid electrolyte (—), an ion–gel electrolyte (– – –), a volatile electrolyte (- - -) and an ionic liquid electrolyte without current collecting grids on a commercial FTO substrate (8–10 Ω/sq) as a reference (– - –).

Table 4
Energy conversion efficiency, η of large sized cells obtained by various electrolyte systems

Electrolyte	Total area, η (%)	Active area, η (%)
Ionic liquid electrolyte	2.3	2.7
Ion–gel electrolyte	2	2.4
Volatile electrolyte	4.3	5.1
Ionic liquid electrolyte without grids[a]	0.2	0.2

[a] As a reference, on a commerical FTO substrate (8–10 Ω/sq).

4. Conclusion

Influence of electrode distance, TiO_2 nano-particle size, thickness of TiO_2 nano-porous layer were investigated in EMIm–TFSA system. J_{sc} remarkably decreased with increasing distance between two electrodes compared with a cell using a volatile electrolyte. Cell performance was more favorable in the case of applying larger size TiO_2 (∅ 13–20 nm). Appropriate condition was considerably different between the ionic liquid electrolyte system and the volatile electrolyte system. At optimized condition, energy conversion efficiency of 4.5% was obtained using a 9 mm × 5 mm small sized cell. In addition, quasi-solidification of the ionic liquid electrolyte was carried out by means of PVdF-HFP as a gelator. Based on those results, ionic liquid

electrolyte type 100 mm × 100 mm large cells were fabricated. Energy conversion efficiency of these cells was 2.7% on the ionic liquid electrolyte system, and 2.4% on the ion–gel electrolyte system (based on active area). At this time, a gap of output between the ionic liquid electrolyte system and the volatile one was so large compared with results obtained by small sized cells owing to some differences about cell fabrication conditions. It was considered that improvement of some matters about cell preparation techniques, such as adhesion of TiO_2 layer, uniformity of coated TiO_2 film thickness, would bring increment of energy conversion efficiency of large sized cells.

Acknowledgements

This work was partially supported by New Energy and Industrial Technology Development Organization (NEDO) under the Japanese government.

References

[1] B. O'Regan, M. Grätzel, Nature 353 (24) (1991) 737.
[2] N. Papageorgiou, Y. Athanassov, M. Armand, P. Bonhôte, H. Pettersson, A. Azam, M. Grätzel, J. Electrochem. Soc. 143 (10) (1996) 3099.
[3] W. Kubo, T. Kitamura, K. Hanabusa, Y. Wada, S. Yanagida, Chem. Commun. (4) (2002) 374.
[4] W. Kubo, S. Kambe, S. Nkakade, T. Kitamura, K. Hanabusa, Y. Wada, S. Yanagida, J. Phys. Chem. B 107 (2003) 4374.
[5] H. Matsumoto, T. Matsuda, T. Tsuda, R. Hagiwara, Y. Ito, Y. Miyazaki, Chem. Lett. (1) (2001) 26.
[6] M. Watanabe, R. Kawano, in: Proceedings of the 201st Meeting of the Electrochemical Society, ECS, Philadelphia, May 2002, p. 1050.
[7] R. Kawano, M. Watanabe, Chem. Commun. (3) (2003) 330.
[8] P. Wang, S.M. Zakeeruddin, I. Exnar, M. Grätzel, Chem. Commun. (24) (2002) 2972.
[9] S. Mikoshiba, H. Sumino, M. Yonetsu, S. Hayase, in: Proceedings of the 16th European Photovoltaic Solar Energy Conference, Glasgow, May 2000, p. 47.
[10] S. Mikoshiba, S. Murai, H. Sumino, S. Hayase, Chem. Lett. (4) (2002) 918.
[11] P. Wang, S.M. Zakeeruddin, P. Comte, I. Exnar, M. Grätzel, J. Am. Chem. Soc. 125 (5) (2003) 1166.
[12] A. Kern, N. van der Burg, G. Chmiel, J. Ferber, G. Hansenhindl, A. Hinsch, R. Kinderman, J. Kroon, A. Meyer, T. Meyer, R. Niepmann, J. van Roosmalen, C. Schill, P. Sommeling, M. Späth, I. Uhlendorf, Opto-Electron. Rev. 8 (4) (2000) 284.
[13] M. Späth, P.M. Sommeling, J.A.M. van Roosmalen, H.J.P. Smit, N.P.G. van der Burg, D.R. Mahieu, N.J. Bakker, J.M. Kroon, Prog. Photovolt.: Res. Appl. 11 (2003) 207.
[14] S. Ito, T. Kitamura, Y. Wada, S. Yanagida, Solar Energy Mater. Solar Cells 76 (2003) 3.
[15] T. Kawashima, H. Matsui, N. Tanabe, Thin Solid Films 445 (2003) 241.
[16] H. Matsui, K. Okada, T. Kawashima, N. Tanabe, Fujikura Gihô 104 (2003) 37.
[17] G. Kron, U. Rau, M. Dürr, T. Miteva, G. Nelles, A. Yasuda, J.H. Werner, Electrochem. Solid-State Lett. 6 (6) (2003) E11.
[18] S.Y. Huang, G. Schlichthörl, A.J. Nozik, M. Grätzel, A.J. Frank, J. Phys. Chem. B 101 (14) (1997) 2576.